

Robust Projection based Anomaly Extraction (RPE) in Univariate Time-Series

Mostafa Rahmani, Anoop Deoras, Laurent Callot

mostrahm@amazon.com

Abstract

This paper presents a novel, closed-form, and data/computation efficient online anomaly detection algorithm for time-series data. The proposed method, dubbed RPE, is a window-based method and in sharp contrast to the existing window-based methods, it is robust to the presence of anomalies in its window and it can distinguish the anomalies in time-stamp level. RPE leverages the linear structure of the trajectory matrix of the time-series and employs a robust projection step which makes the algorithm able to handle the presence of multiple arbitrarily large anomalies in its window. A closed-form/non-iterative algorithm for the robust projection step is provided and it is proved that it can identify the corrupted time-stamps. RPE is a great candidate for the applications where a large training data is not available which is the common scenario in the area of time-series. An extensive set of numerical experiments show that RPE can outperform the existing approaches with a notable margin.

I. INTRODUCTION

Anomaly detection is an important research problem in unsupervised learning where the main task is to identify the observations which do not follow the common structure of the data. Anomalies mostly correspond to rare but important events whose detection is of paramount importance. For instance, in medical imaging, the outlying patches could correspond to malignant tissues [Karrila et al., 2011], and in computer networks an anomaly can imply an intrusion attack [Kruegel and Vigna, 2003].

In many applications and businesses, the given data is a time-series of real values where each value represents the value of an important metric/sensor/measurement at a time-stamp and the values are mostly sampled with a fixed frequency [Braei and Wagner, 2020]. In these applications, it is important to identify if (based on the past observation) a given time-stamp value is an anomaly or if it is a part of an anomalous pattern. An anomaly detection algorithm for time-series data is preferred to have two desirable properties: **(a)** The algorithm should be able to declare an anomaly without any delay. In other word, the algorithm only relies on the past observations.

(b) If an anomaly happens in time-stamp t , the algorithm should only label time-stamp t as anomalous and the anomaly label should not be diffused to the neighboring time-stamps. We will discuss this important property further in the next sections since most window-based methods [Braei and Wagner, 2020], [Guha et al., 2016], [Ren et al., 2019] can keep reporting anomalies for a long period of time after the anomaly occurred, as long as their window contains the anomaly.

This paper presents a new window-based algorithm which, in sharp contrast to the current window-based methods, is provably robust to the presence of anomalies in its window. The algorithm, dubbed RPE, can distinguish outlying behaviors at the time-stamp level. The main contributions of this work can be summarized as follows.

- We present an accurate and data/computationally efficient algorithm which is based on transforming the problem of anomaly detection in uni-variate time series into the problem of robust projection into a linear manifold.
- To the best of our knowledge, RPE is the only window-based method which is provably robust to the presence of outlying time-stamps in its window.
- The projection step involves solving a convex optimization problem. A closed form method is proposed which saves the algorithm from running an iterative solver for each time-stamp.
- Novel theoretical results are established which guarantee the performance of the projection step.
- An extensive set of experiments with real/synthetic data show that RPE can notably outperform the former approaches.

A. Definitions and notation

Bold-face upper-case and lower-case letters are used to denote matrices and vectors, respectively. For a vector \mathbf{a} , $\|\mathbf{a}\|_p$ denotes its ℓ_p -norm, $\mathbf{a}(i)$ denotes its i^{th} element, and $|\mathbf{a}|$ is a vector whose values are equal to the absolute value of the corresponding elements in \mathbf{a} . Similarly, the elements of $\mathbf{Y} = |\mathbf{X}|$ are equal to the absolute value of the elements of matrix \mathbf{X} . For a matrix \mathbf{A} , \mathbf{A}^T is the transpose of \mathbf{A} and \mathbf{a}_i indicates the i^{th} row of \mathbf{A} . \mathbb{S}^{M_1-1} indicates the unit ℓ_2 -norm sphere in \mathbb{R}^{M_1} . Subspace \mathcal{U}^\perp is the complement of \mathcal{U} . For a set \mathcal{I} , $|\mathcal{I}|$ indicates the cardinality of \mathcal{I} .

The coherency of a subspace \mathcal{U} with the standard basis is a measure of the sparsity of the vectors which lie in \mathcal{U} [Chandrasekaran et al., 2011], [Candès and Recht, 2009]. The following definition provides three metrics which can represent the coherency of a linear subspace.

Definition 1. Suppose $\mathbf{U} \in \mathbb{R}^{M_1 \times r}$ is an orthonormal matrix. Then we define

$$\begin{aligned}\mu^2(\mathbf{U}) &= \max_i \frac{\|\mathbf{e}_i^T \mathbf{U}\|_2^2}{r}, \\ \gamma(\mathbf{U}) &= \frac{1}{\min_{\mathbf{h} \in \mathbb{S}^{r-1}} \|\mathbf{U} \mathbf{h}\|_1}, \\ \kappa(\mathbf{U}) &= \mu(\mathbf{U})\gamma(\mathbf{U}),\end{aligned}\tag{1}$$

where \mathbf{e}_i is the i^{th} row of the identity matrix.

The parameter $\mu^2(\mathbf{U})$ shows how close \mathcal{U} (the column space of \mathbf{U}) is to the standard basis and $\gamma(\mathbf{U})$ measures the minimum of the ℓ_1 -norm of all the vectors on the intersection of \mathbb{S}^{r-1} and \mathcal{U} . Clearly, the more sparse are the vectors in \mathcal{U} , the larger are $\mu^2(\mathbf{U})$ and $\gamma(\mathbf{U})$.

Suppose we have a set of samples from a random variable saved in set \mathcal{M} . The empirical CDF value corresponding to a sample x is defined as $\frac{|\mathcal{M} < x|}{|\mathcal{M}|}$ where $|\mathcal{M} < x|$ is the number of elements in \mathcal{M} which are smaller than x and $|\mathcal{M}|$ is the size of \mathcal{M} . The trajectory matrix $\mathbf{X} \in \mathbb{R}^{M_1 \times (n - M_1 + 1)}$ corresponding to time-series $\mathbf{t} \in \mathbb{R}^n$ is defined as

$$\mathbf{X} = \begin{bmatrix} \mathbf{t}(1) & \mathbf{t}(2) & \dots & \mathbf{t}(n - M_1 + 1) \\ \mathbf{t}(2) & \mathbf{t}(3) & \dots & \mathbf{t}(n - M_1 + 2) \\ \vdots & \vdots & & \vdots \\ \mathbf{t}(M_1) & \mathbf{t}(M_1 + 1) & \dots & \mathbf{t}(n) \end{bmatrix},$$

where M_1 is the size of the running window and define $M_2 = n - M_1 + 1$ (\mathbf{X} is created by running a window of size M_1 on \mathbf{t}).

II. RELATED WORK

The simplest method to identify outlying time-stamps in a time-series is to treat the time-stamp values as independent samples from a probability distribution (e.g., Gaussian) and infer the distribution from the former samples. In this paper, we refer to this approach as IID. IID can successfully identify the anomalies whose time-stamp values are outside of the range of the values of normal time-stamps. However, IID is completely blind in identifying the contextual anomalies which do not necessarily push the value outside of the normal range of the values. It is not a proper assumption in many time-series to presume that time-stamp values are independent as time-series frequently have an underlying structure, for example seasonality.

A popular approach to utilize the structure of the time-series is to have a running window which provides the opportunity to compare the local structure of the time-series against the past observations to decide if there is an anomaly in the given window. Some of the window-based methods are Random

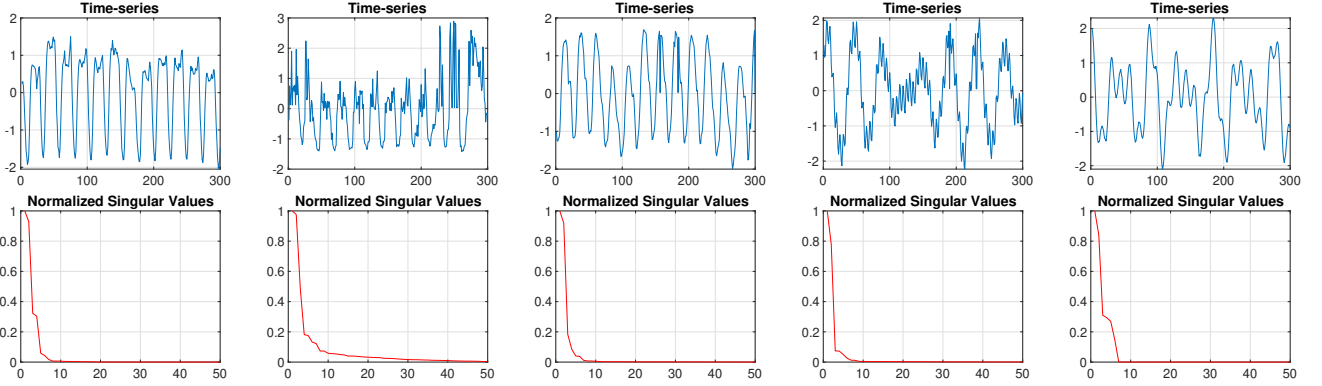


Fig. 1. This plot shows 5 normalized time-series where the first three time-series (from left) are sampled from real data (Yahoo dataset) and the last two time-series are synthetic. The second row demonstrates the normalized eigenvalues of the covariance matrix of the corresponding trajectory matrices. One can observe that the eigenvalues drop rapidly which suggests that the trajectory matrices can be accurately approximated using a low rank matrix.

Cut Forest (RCF) [Guha et al., 2016], Auto-Regressive (AR) model [Braei and Wagner, 2020], and the Spectral Residual (SR) based method [Ren et al., 2019].

Another approach to infer the underlying structure of the data is to employ a deep neural network [Shen et al., 2020], [Zhao et al., 2020], [Su et al., 2019], [Hundman et al., 2018], [Munir et al., 2018], [Zhou et al., 2019], [Xu et al., 2018], [Challu et al., 2022]. However, deep learning methods are not applicable in many applications where there is not enough data to train the network, this is particularly common for low-frequency time-series data.

In this paper, we focus on the scenarios where only a short history for a single time-series is available.

The lines of work most closely related to this paper are singular spectrum based time-series analysis [Dokumentov et al., 2014], [Golyandina et al., 2001], [Papailias and Thomakos, 2017], [Khan and Poskitt, 2017] and robust matrix decomposition [Candès et al., 2011], [Chandrasekaran et al., 2011] which we discuss in the following sections.

A. Singular spectrum analysis

Low-rank representations and approximations have been shown to be a very useful tool in time series analysis. One of the popular approaches is singular spectrum analysis that represents the time-series using the trajectory matrix and uses a low-rank approximation to model the time-series and the model is used to compute the next values of a time series [Dokumentov et al., 2014], [Golyandina et al., 2001], [Papailias and Thomakos, 2017], [Khan and Poskitt, 2017]. Singular spectrum analysis uses the fact that

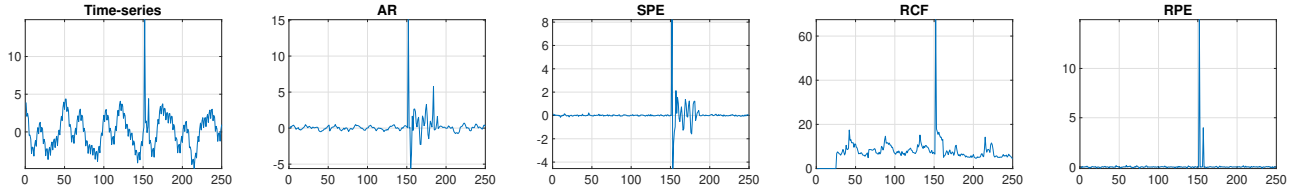


Fig. 2. The first plot (from left) shows the time-series which includes two anomalies at indices 151 and 156. The next 4 plots demonstrate the anomaly scores computed by 4 window-based methods. SPE (Simple Projection based anomaly Extraction) is similar to RPE but it employs a simple projection instead of the robust projection step employed in RPE.

many time series can be well approximated by a class of so-called time series of finite rank [Usevich, 2010], [Gillard and Usevich, 2018], [Golyandina et al., 2001]. Finite rank time-series is a time-series whose trajectory matrix is a low rank matrix. The real valued time-series of finite rank can be written as the sums of products of cosines, exponential and polynomial functions as $\mathbf{t}(k) = \sum_{j=1}^{s_1} Q_j(k) \rho_j^k \cos(2\pi\omega_j k + \phi_j) + \sum_{j=s_1+1}^{s_2} Q_j(k) \rho_j^k$, where $Q_j(k)$ are real polynomials of degrees $\mu_j - 1$, $\omega_j \in (0, 0.5)$, and $\phi_j \in \mathbb{R}$, $\rho \in \mathbb{R}$ are distinct numbers and the pairs $\{(\rho_j, \omega_j)\}_{j=1}^{s_1}$ are also distinct [Gillard and Usevich, 2018]. This class of time-series can accurately model trends, periodicities and modulated periodicities in time series [Golyandina et al., 2001] and the rank of the trajectory matrix is equal to $r = \sum_{j=1}^{s_1} 2\mu_j + \sum_{j=s_1+1}^{s_2} \mu_j$ if $M_1, M_2 > r$ [Usevich, 2010]. Figure 1 shows few real and synthetic time-series along with the singular spectrum of their corresponding trajectory matrices. The curve of the singular values show that the trajectory matrices can be accurately approximated using low rank matrices. The authors of [Gillard and Usevich, 2018], [Usevich and Comon, 2016] leveraged the low rank structure of the trajectory matrix to employ matrix completion techniques [Candès and Recht, 2009], [Lois and Vaswani, 2015] to perform time-series forecasting and missing value imputation.

B. Anomaly detection using robust PCA

An interesting topic in the literature of robust PCA is the problem of low rank plus sparse matrix decomposition where the given data matrix \mathbf{D} is assumed to be a summation of an unknown low rank matrix and an unknown sparse matrix [Candès et al., 2011], [Chandrasekaran et al., 2011], [Feng et al., 2013]. A convex optimization based solution to this problem was proposed in [Candès et al., 2011], [Chandrasekaran et al., 2011] and the authors established sufficient conditions under which the algorithm is guaranteed to decompose the data exactly with high probability. Since the trajectory matrix of time-series with a background signal can mostly be approximated using a low rank matrix, one can consider the trajectory matrix of the time-series in the presence of anomalies as the summation of a low rank matrix and a sparse matrix. This observation

motivated [Jin et al., 2017], [Wang et al., 2018] to employ the matrix decomposition algorithm analyzed in [Candès et al., 2011], [Chandrasekaran et al., 2011], [Rahmani and Atia, 2017b] for anomaly detection in time-series data. However, the methods proposed in [Jin et al., 2017], [Wang et al., 2018] require solving the nuclear norm based optimization problem in each time-stamp whose solver requires computing a SVD of an $M_1 \times M_2$ dimensional matrix per iteration which means that the computation complexity of processing a single time-stamp is $\mathcal{O}(M_1^2 M_2 k)$ where k is the number of iterations it takes for the solver to converge. In this paper, we also utilize the underlying linear structure of the trajectory matrix but we transform the decomposition problem into a robust projection problem and a closed-form algorithm is presented which saves the algorithm from the complexity of running an iterative solver for every time-stamp.

III. MOTIVATION: THE PROBLEM OF WINDOW-BASED METHODS

Many of the time-series anomaly detection algorithms are window-based methods (e.g., SR, AR, RCF, ...). Although with a window of samples we move the problem into a higher dimensional space where the anomalous pattern are more separable, window-based methods suffer from two main setbacks:

- The window-based methods which rely on using an unsupervised outlier detection method (e.g., RCF [Guha et al., 2016]) are partially or completely blind about the location of the anomaly in their window. This shortcoming might cause the algorithm to report a single anomaly for a long period time (as long as the anomaly is present in the window).
- Some of the window-based methods (such as AR and SR) uses the samples in the window to compute a residual value corresponding to each time-stamp which is the difference between the actual value and the forecast value. These algorithms are not robust to the presence of anomalies in the window and the presence of anomalies in the window can cause significant error in the computed residual value.

The main contribution of this work is proposing an efficient and closed-form window-based method which is robust to the presence of anomalies in its window. Figure 2 shows the anomaly scores computed using 4 window-based methods. The time-series includes two anomalies at indices 151 and 156 and the size of window is equal to 30. One can observe RPE precisely distinguished the two anomalies and the presence of anomalies did not affect the residual values of the neighboring time-stamps. In contrast, with the other methods, we observe two major problems. First, the strong anomaly masked the weaker anomaly; second, the presence of anomalies in the window caused the algorithms to generate high anomaly scores for a long period of time.

Algorithm 1 RPE for anomaly detection in univariate time-series

Input: Training time-series $\mathbf{t}_{tr} \in \mathbb{R}^n$, retraining frequency q , window size M_1 , and max training size t_{\max} .

1. Training

1.1 If the length of \mathbf{t}_{tr} is larger than t_{\max} , discard the first $n - t_{\max}$ samples.

1.2 Build trajectory matrix $\mathbf{X} \in \mathbb{R}^{M_1 \times M_2}$ using \mathbf{t}_{tr} .

1.3 Apply the robust subspace recovery algorithm to \mathbf{X} to estimate \mathcal{U} and define $\mathbf{U} \in \mathbb{R}^{M_1 \times r}$ as an orthonormal basis for \mathcal{U} .

Remark. The rank of \mathbf{X} is estimated by the subspace recovery algorithm.

1.5 Set counter $c = 0$.

2. Online Inference. For any new time-stamp value v :

2.1 Append v to \mathbf{t}_{tr} and update $c = c + 1$.

2.2 Build $\mathbf{x} \in \mathbb{R}^{M_1}$ using the last M_1 elements of \mathbf{t}_{tr} .

2.2 Use Algorithm 2 (robust projection) to compute $\hat{\mathbf{a}}$.

2.3 Compute the residual value corresponding to v as $e = v - \hat{\mathbf{a}}^T \mathbf{u}_{-1}$ where \mathbf{u}_{-1} is the vector of the last row of \mathbf{U} .

2.4 If the remainder of $\frac{c}{q}$ is equal to 0, perform Step 1.1, Step 1.2, and Step 1.3 to update \mathbf{U} .

IV. PROPOSED APPROACH

Detecting anomalies in time-series with a background pattern can be challenging since the value of an anomalous time-stamp can lie in the range of normal values, which means that thresholding-based methods such as the IID method or the method discussed in [Siffer et al., 2017] are not able to identify the outlying time-stamps. In Section II-A we discussed how the trajectory matrix of a time-series with a background pattern can mostly be approximated using a low dimensional linear model [Gillard and Usevich, 2018], [Papailias and Thomakos, 2017]. The main idea behind the RPE algorithm is to utilize the linear model to extract the outlying component of each time-stamp value. We propose to employ a robust projection step which makes the presented method robust against the presence of anomalies in its window and it enables the algorithm to distinguish anomalies at the time-stamp level. A closed-form and provable algorithm is presented to perform the robust projection step.

Remark 1. We assume that the given time-series \mathbf{t} can be written as $\mathbf{t} = \mathbf{t}_b + \mathbf{t}_s + \mathbf{t}_n$ where \mathbf{t}_b is the background signal, \mathbf{t}_s represents the outlying components of the time-stamps (\mathbf{t}_s is assumed to be a

sparse vector) and \mathbf{t}_n is the additive noise. In the next section, it is assumed that the orthonormal matrix $\mathbf{U} \in \mathbb{R}^{M_1 \times r}$ defined as the span of the column space of the trajectory matrix of \mathbf{t}_b is given. Subsequently, we discuss efficient algorithms which can accurately estimate \mathbf{U} from the trajectory matrix of the training time-series.

Algorithm 2 Robust Linear Projection

Input: The orthonormal matrix $\mathbf{U} \in \mathbb{R}^{M_1 \times r}$, the observation vector \mathbf{x} , and n_s as an upper-bound on the number of corrupted elements of \mathbf{x} .

1. Define $\hat{\mathbf{e}} = |\mathbf{x} - \mathbf{U}\mathbf{U}^T\mathbf{x}|$.
2. Define set \mathcal{I} with cardinality $M_1 - n_s$ as the indices of the elements of $\hat{\mathbf{e}}$ with the smaller values.
3. Define $\mathbf{U}_{\mathcal{I}} \in \mathbb{R}^{(M_1 - n_s) \times r}$ as the rows of \mathbf{U} whose indices are in \mathcal{I} and define $\mathbf{x}_{\mathcal{I}}$ similarly.

Output: $\hat{\mathbf{a}} = (\mathbf{U}_{\mathcal{I}}^T \mathbf{U}_{\mathcal{I}})^{-1} \mathbf{U}_{\mathcal{I}}^T \mathbf{x}_{\mathcal{I}}$.

A. Robust projection for anomaly detection in time-series

It is assumed that the trajectory matrix of \mathbf{t}_b can be accurately described using a low dimensional linear subspace \mathcal{U} spanned by \mathbf{U} . Therefore, each window $\mathbf{x} \in \mathbb{R}^{M_1}$ can be written as

$$\mathbf{x} = \mathbf{U}\mathbf{a} + \mathbf{s} + \mathbf{n}, \quad (2)$$

where \mathbf{s} and \mathbf{n} represent the components corresponding to anomalies and noise, respectively. In order to simplify the following discussion, let us temporarily ignore the presence of the added noise and presume that

$$\mathbf{x} = \mathbf{U}\mathbf{a} + \mathbf{s}. \quad (3)$$

We would like to estimate \mathbf{s} to identify the anomalous time-stamps. A simple solution is to simply project \mathbf{x} into the column space of \mathbf{U} which means that \mathbf{s} is estimated as $\hat{\mathbf{s}} = \mathbf{x} - \mathbf{U}\hat{\mathbf{a}}$ where $\hat{\mathbf{a}}$ is the optimal points of

$$\arg \min_{\hat{\mathbf{a}}} \|\mathbf{x} - \mathbf{U}\hat{\mathbf{a}}\|_2 = \mathbf{U}^T \mathbf{x}. \quad (4)$$

The algorithm based on (4), which we call it Simple Projection based anomaly Extraction (SPE), is still one of the best algorithms for anomaly detection in the time-series with a back-ground signal. However, the estimation obtained by (4) is the optimal point of the likelihood function when we model the elements of \mathbf{s} as independent samples from a zero mean Gaussian distribution. This is an obviously

wrong assumption given that \mathbf{s} is known to be a sparse vector (i.e., the anomalies corrupt few time-stamps) and the non-zero elements of \mathbf{s} can have arbitrarily large values. It is well known that ℓ_1 -norm is robust to the presence of sparse corruptions [Candes and Tao, 2005], [Candès et al., 2011]. The authors of [Candes and Tao, 2005] provided the sufficient conditions which guarantee that the optimal point of

$$\arg \min_{\hat{\mathbf{a}}} \|\mathbf{x} - \mathbf{U}\hat{\mathbf{a}}\|_1 \quad (5)$$

is equal to \mathbf{a} . The key factors to ensure the success of (5) are that the column-space of \mathbf{U} should not include sparse vectors and \mathbf{s} should be sufficiently sparse. In order to show the dependency on these two important factors, we derived the following new guarantee whose sufficient condition is more insightful in showing the dependency on the incoherency of \mathcal{U} (the proof is also easier). In the next section, we show that the incoherency of \mathcal{U} can be leveraged to design a provable closed-form algorithm.

Lemma 1. *Suppose vector $\mathbf{x} \in \mathbb{R}^{M_1}$ is generated as $\mathbf{x} = \mathbf{U}\mathbf{a} + \mathbf{s}$ where $\mathbf{U} \in \mathbb{R}^{M_1 \times r}$ and vector \mathbf{s} contains m non-zero elements. If*

$$\kappa(\mathbf{U}) < \frac{1}{2m\sqrt{r}}, \quad (6)$$

then $\hat{\mathbf{a}}$ is the optimal point of (5).

Lemma 1 indicates that if \mathcal{U} is sufficiently incoherent and \mathbf{s} is sparse enough, then \mathbf{a} can be perfectly recovered, no matter how large the non-zero elements of \mathbf{s} are. This feature enables the anomaly detection algorithm to achieve high accuracy in the point-wise detection of anomalous time-stamps. In online anomaly detection, the last element of $\mathbf{x} - \mathbf{U}\hat{\mathbf{a}}$ is the residual value of the last received time-stamp. Lemma 1 indicates that *even if the window contains $m - 1$ anomalies, the residual value computed by (5) is not influenced by them.* This is the main motivation that in this paper we propose to employ a robust projection algorithm to compute the residual values.

B. The closed-form solver for the robust projection step

In section IV-A, we proposed to utilize the linear structure of the trajectory matrix and employ the robust projection based on (5) to compute the residual values since it ensures that an anomaly only affects the residual value of its corresponding time-stamp which leads to achieving high detection accuracy. However, the optimization problem (5) does not have a closed-form solution and one needs to employ an iterative solver to find the optimal point for each time-stamp.

The following lemma reveals the key idea to design a closed form solution. It shows that if \mathcal{U} is sufficiently incoherent and \mathbf{s} is sparse enough, then the residual values computed based on (4) can be used to find a set of candidate indices of the corrupted time-stamps.

Remark 2. In the following lemma, in order to simplify the exposition of the result, it is assumed that the absolute value of the non-zero elements of \mathbf{s} are equal. This assumption is not important in the performance of the algorithm and the full result without the assumption along with the proof is available in the appendix.

Lemma 2. Suppose \mathbf{x} is generated as in Lemma 1, assume the absolute value of the non-zero elements of \mathbf{s} are equal to τ , define $\hat{\mathbf{e}} = |\mathbf{x} - \mathbf{U}\mathbf{U}^T\mathbf{x}|$, and define \mathcal{I}_s as the set of indices of the non-zero elements of \mathbf{s} . If

$$\mu^2(\mathbf{U}) \leq \frac{1}{2 r m}, \quad (7)$$

then $\min_{i \in \mathcal{I}_s} \hat{\mathbf{e}}(i) > \max_{i \notin \mathcal{I}_s} \hat{\mathbf{e}}(i)$, where $m = |\mathcal{I}_s|$.

Importantly, Lemma 2 indicates that although the residual values computed using (4) are faulty (a single anomaly can cause significant residual values in all the time-stamps of the window), they can be used to identify the potentially corrupted time-stamps. Based on Lemma 2, the following corollary can be concluded.

Corollary 3. Define $\hat{\mathbf{e}}$ as in Lemma 2 and define set \mathcal{I}_c with $|\mathcal{I}_c| = n_s > m$ as the set of indices of $\hat{\mathbf{e}}$ with the largest elements where $|\mathcal{I}_c|$ is the cardinality of \mathcal{I}_c . Form matrix $\mathbf{U}_{\mathcal{I}_c^\perp} \in \mathbb{R}^{(M_1 - n_c) \times r}$ using the rows of \mathbf{U} whose indices are not in \mathcal{I}_c and define $\mathbf{x}_{\mathcal{I}_c^\perp}$ similarly. In addition, suppose $\text{rank}(\mathbf{U}_{\mathcal{I}}) = r$ for any set of indices with $|\mathcal{I}| = n_s$. If (7) holds, then

$$(\mathbf{U}_{\mathcal{I}_c^\perp}^T \mathbf{U}_{\mathcal{I}_c^\perp})^{-1} \mathbf{U}_{\mathcal{I}_c^\perp}^T \mathbf{x}_{\mathcal{I}_c^\perp} = \mathbf{a}. \quad (8)$$

It is important to note that τ does not appear in the sufficient condition which means no matter how large are the anomalies, the proposed method is guaranteed to recover \mathbf{a} correctly. Lemma 2 and Corollary 3 showed that the incoherency of \mathbf{U} imposed an structure on the residual values computed using (4) such that we can filter out the potentially corrupted observations and compute the correct \mathbf{a} in a closed form way. The following theorem states that the estimation error is proportional to the variance of the noise if the observation vector \mathbf{x} contains additive noise.

Theorem 4. Suppose $\mathbf{x} = \mathbf{U}\mathbf{a} + \mathbf{s} + \mathbf{n}$ where \mathbf{U} and \mathbf{s} are as in Lemma 2 and $\mathbf{n} \sim \mathcal{N}(\mathbf{0}, \sigma_n^2 \mathbf{I})$ is the added Gaussian noise and define η such that $\mathbb{P}[|\mathbf{n}(i)| > \eta] < \frac{\delta}{M_1}$. In addition, suppose $\text{rank}(\mathbf{U}_{\mathcal{I}}) = r$

for any set of indices with $|\mathcal{I}| = n_s$ where $n_s > m$ and $m = |\mathcal{I}_s|$. Define $\mathbf{U}_{\mathcal{I}_c^\perp}$ as in Corollary 3 and define $\hat{\mathbf{a}} = (\mathbf{U}_{\mathcal{I}_c^\perp}^T \mathbf{U}_{\mathcal{I}_c^\perp})^{-1} \mathbf{U}_{\mathcal{I}_c^\perp}^T \mathbf{x}_{\mathcal{I}_c^\perp}$. If

$$\mu^2 \left(1 + \frac{\eta}{m\tau} \sqrt{\frac{M_1 \log 1/\delta}{2}} \right) \leq \frac{1}{2r m}, \quad (9)$$

then $\hat{\mathbf{a}}$ is an unbiased estimate of \mathbf{a} and the variance of $\hat{\mathbf{a}}(i)$ is smaller than σ_n with probability at least $1 - 2\delta$.

The sufficient condition states that \mathbf{U} should be sufficiently incoherent with the standard basis. Matrix \mathbf{U} spans the column space of the trajectory matrix \mathbf{X} and it means that RPE can successfully compute the residual values if the given time-series is not sparse (the column space of \mathbf{X} does not contain sparse vectors). In addition, the sufficient condition requires $m = |\mathcal{I}_s|$ to be small enough which means that the corrupted elements should not dominate \mathbf{x} .

Algorithm 1 presents the RPE algorithm and Algorithm 2 demonstrates the closed form robust projection step. Algorithm 2 uses n_s as an upper-bound on the number of anomalies which can be present in window \mathbf{x} . Normally a small portion of the time-stamps are anomalous and a small value for n_s (e.g., $0.05 M_1$) is sufficient.

Algorithm 1 includes a retraining logic which uses the accumulated samples of the time-series to update the estimation of \mathbf{U} . This is helpful for the low data regimes to keep improving the estimate of \mathbf{U} and it can be ignored if the given \mathbf{t}_{tr} is long enough. In our experiments, we turned off the retraining logic when the length of \mathbf{t}_{tr} becomes larger than $10M_1$. In addition, in the special scenarios where the background pattern could change through time, the retraining logic can be employed to update \mathbf{U} with a proper frequency.

Similar to several other window-based methods, the output of Algorithm 1 is the computed residual values. In this paper, we directly apply a threshold to the computed residual values to compute the accuracy of the model. One can convert the computed residual values to probabilistic scores via inferring the distribution of the generated residual values. In addition, in the applications where the user can provide feedback, dynamic thresholding can be utilized to learn the user's desired detection rate [Raginsky et al., 2012].

1) *Robust estimating of \mathcal{U} :* In the presumed data model, we assumed that the given time-series can be written as $\mathbf{t} = \mathbf{t}_b + \mathbf{t}_s + \mathbf{t}_n$ which means that $\mathbf{X} = \mathbf{B} + \mathbf{S} + \mathbf{N}$ where \mathbf{X} is the trajectory matrix of \mathbf{t} and \mathbf{B} , \mathbf{S} , and \mathbf{N} are the components corresponding to \mathbf{t}_b , \mathbf{t}_s , and \mathbf{t}_n , respectively. Since \mathbf{B} is a low rank matrix for most of the background signals, the robust matrix decomposition algorithm studied in [Chandrasekaran et al., 2011] can be employed to recover \mathbf{B} from \mathbf{X} and \mathcal{U} can be estimated as

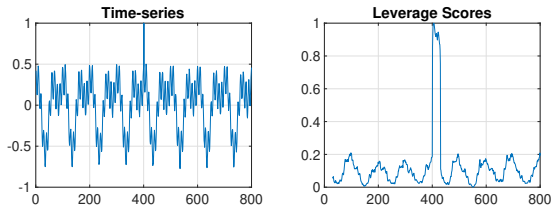


Fig. 3. The left plot shows a time-series which includes one anomaly. The right plot shows leverage scores where each score corresponds to one column of the trajectory matrix. In this example, if we filter out a small portion of the columns of \mathbf{X} corresponding to the largest leverage scores, \mathbf{X} will be free of outlying columns.

the column space of the recovered \mathbf{B} . However, the method proposed in [Chandrasekaran et al., 2011] involves solving an optimization problem which requires running an iterative solver for many iterations. In time-series, a small portion (mostly less than 1 %) of the time-stamps are anomalies and in this section, we discuss techniques which leverage the sparsity of the anomalies to estimate \mathcal{U} efficiently. We discuss three approaches to filter out the outlying components from \mathbf{X} to estimate the column space of \mathbf{B} from the filtered/cleaned \mathbf{X} .

- *Column-wise approach:* In the scenarios where $n \gg M_1$ and a small portion of the elements of \mathbf{t} are anomalies, a small portion of the columns of \mathbf{X} contain the outlying time-stamps and we can employ a column-wise anomaly detection algorithm such as leverage score or the methods proposed in [Lerman and Maunu, 2018], [Rahmani and Li, 2019], [Rahmani and Atia, 2017a], [Rahmani and Li, 2021] to identify them (the columns which contain anomalies) and filter them from \mathbf{X} . The remaining clean columns can be used to estimate \mathbf{U} . If we utilize leverage scores to identify the outlying columns of \mathbf{X} , the computation complexity of this step is $\mathcal{O}(M_1 M_2 r)$. Figure 3 shows an illustrative example.

- *Element-wise approach:* The first discussed technique was based on the idea of filtering out the outlying columns of the trajectory matrix. However, when n is not significantly larger than M_1 , a single outlying time-stamp appears in a large portion of the columns of \mathbf{X} and one can not filter out the anomalies via removing a small portion of the columns of \mathbf{X} . The second technique is based on identifying the outlying elements of \mathbf{X} and replacing them with the estimated values. Algorithm 3 leverages the fact that when a small portion of the elements of \mathbf{X} are anomalies, the span of the dominant left singular vectors of \mathbf{X} are close to \mathcal{U} (the column space of \mathbf{B}). Algorithm 3 replaces a small portion of the elements of \mathbf{X} (the elements with the largest absolute values) with the median value to make the initial estimate of \mathcal{U} robust to arbitrary large anomalies. Next, the algorithm utilizes the estimated \mathcal{U} to identify the candidate outlying elements to update the estimation of \mathcal{U} . The computation complexity of Algorithm 3 is $\mathcal{O}(M_1 M_2 r)$.

• *Simple approach:* In most of applications, a small portion of the time-stamp values are outliers (mostly less than 1 %). However, the value of the outlying time-stamps could be significantly large such that their presence in \mathbf{X} could deviate the span of the major principal components of \mathbf{X} from \mathcal{U} . Contextual anomalies have a negligible impact on the major principal components of \mathbf{X} and in order to tackle the impact of the anomalies with large time-stamp values, Algorithm 4 replaces a small portion of the time-stamp values (which have the largest absolute values) with the median value of the given time-series (median is robust to the presence of anomalies). Although we are not replacing those values with the correct values, its impact on the performance of the algorithm is negligible since we are replacing a small portion of the time-stamp values (β can be chosen less than 1 in most applications). This simple technique can ensure that \mathbf{X} does not contain outlying elements with arbitrary large values and we can rely on the principal components of \mathbf{X} to obtain \mathbf{U} . In our investigations, we observed that this simple method (Algorithm 4) performs as well as Algorithm 3 in most cases and we used it in the presented experiments to estimate \mathcal{U} .

Remark 3. *Different methods can be used to choose r . In this paper, we set r equal to number of the singular values which are greater than $s_1/100$ where s_1 is the first singular value. Another approach is to choose the rank based on $\frac{\|\mathbf{X} - \mathbf{U}\mathbf{U}^T\mathbf{X}\|_F}{\|\mathbf{X}\|_F}$ where $\|\mathbf{X}\|_F$ is the Frobenius norm of \mathbf{X} .*

Algorithm 3 Robust estimation of \mathcal{U} (element-wise approach)

Input: The given time-series \mathbf{t} and parameter α .

1. Form \mathbf{X} as the trajectory matrix of \mathbf{t} .
2. Select α percent of the elements of \mathbf{t} with highest absolute values and replace their values with the median value \mathbf{t} . In addition, define \mathbf{Q} as the trajectory matrix of the updated \mathbf{t} .
3. Define \mathbf{U} as the matrix of first r left singular vectors of \mathbf{Q} .
- 4 Replace the potential anomalies with the estimated values:
 - 4.1 Define $\mathbf{E} = |\mathbf{X} - \mathbf{U}\mathbf{U}^T\mathbf{X}|$.
 - 4.2 Define \mathcal{I}_o as the set of indices of α percent of the elements of \mathbf{E} with the highest values.
 - 4.3 Replace the elements of \mathbf{X} whose indices are in \mathcal{I}_o with the corresponding values in matrix $\mathbf{U}\mathbf{U}^T\mathbf{Q}$.
5. Update \mathbf{U} as the matrix of first r left singular vectors of the updated \mathbf{X} .

Output: Matrix \mathbf{U} .

Algorithm 4 Robust estimation of \mathcal{U} (simple approach)**Input:** The given time-series \mathbf{t} and parameter β (e.g., $\beta = 1$).

1. Define \mathcal{I}_m as the indices of $\beta\%$ of elements of \mathbf{t} with the largest absolute values.
2. Replace the values of the elements of \mathbf{t} whose indices are in \mathcal{I}_m with the median value of \mathbf{t} .
3. Form \mathbf{X} as the trajectory matrix of \mathbf{t} .
4. Define \mathbf{U} as the matrix of first r left singular vectors of \mathbf{X} .

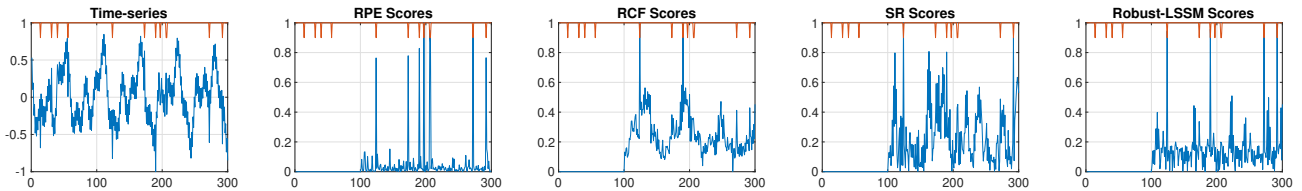
Output: Matrix \mathbf{U} .

Fig. 4. This figure shows a time-series with several contextual anomalies as described in Section V-A1. The red lines in each plot indicates the location of the outlying time-stamps. The plotted scores indicate that RPE successfully identifies even the weak anomalies. Each algorithm used the first 100 time-stamps as training data (refer to Section V-A1 for further details).

V. NUMERICAL EXPERIMENTS

In this section, we compare the performance of the proposed approach against popular alternatives applicable in low data regimes where we have a limited number of samples from a time-series for training (in all the presented experiments, we provide no more than 100 training time-stamps). The methods that we compare against include Random Cut Forest (RCF) [Guha et al., 2016], Robust Linear State Space Model (LSSM) [Durbin and Koopman, 2012], Spectral Residual (SR) [Ren et al., 2019], IID, Autoregressive model [Chandola, 2009], and Simple Projection based anomaly Extraction (SPE). The size of the window is set equal to 30 in all the experiments.

In the RCF method, we set the number of trees equal to 30, and the sample size equal to 256. In the IID method, a memory of 100 last observed values is used to compute the mean and the variance which are then used to compute the p-value of each observation value based on Gaussian distribution. The anomaly score is equal to $1 - p$ where p is the p-value. The Robust LSSM algorithm is a Linear Gaussian State Space Model equipped with dynamic masking where the algorithm considers the observations whose likelihood values are small as missing values and those observations are not used to perform filtering in the Kalman Filter. Specifically, we compute the empirical CDF value of each generated score by the LSSM model using the memory of previously generated scores and those observations whose empirical CDF values are larger than 0.95 were not used to filter the state of the model. This technique helps the

model to generate sharp anomaly scores. The used parameters for the RPE algorithm in all the presented experiments are $M_1 = 30$, $q = 100$, $t_{\max} = 300$, and $n_s = 5$.

The SPE algorithm is similar to the proposed RPE algorithm with only one difference. The difference is that SPE employs a simple projection method to compute the residual values corresponding to each observation vector. The SR algorithm requires computing Fast Fourier Transform (FFT) and inverse FFT for each time-stamp to compute the residual value. The length of the widow used for the computation of FFT was chosen equal to 128.

Remark 4. *We set r to equal the number of the singular values of $\mathbf{X}\mathbf{X}^T$ which are greater than $s_1/100$ where s_1 is the largest singular value of $\mathbf{X}\mathbf{X}^T$. If the estimated rank is larger than 10 (which can happen for random time-series that do not contain a background temporal pattern), we set $r = 10$.*

Remark 5. *In the experiments below all the models are trained locally, a separate model is trained for each time-series. This is a more realistic setting for many applications where we do not have a large number of related time-series. For instance, if a dataset contains 5 time-series and the AR algorithm is used, the AR algorithm learns a different weight vector for each time-series.*

Ablation study: The key component of the proposed method which distinguishes it from the Singular spectrum analysis based algorithms is the robust projection step and its closed form implementation. In order to show its significance, we included the performance of SPE in all the presented experiments. The performance of SPE shows the performance of RPE in absence of the robust projection step.

Probabilistic scores: In some applications, the anomaly detection algorithm is required to provide probabilistic anomaly scores (e.g, one minus p-value). Similar to most other anomaly detection algorithms (e.g., RCF, SR), RPE does not generate probabilistic scores and its outputs are the residual values. RPE transforms the given time-series with a possibly complicated background pattern into a simple series of residual values where the anomalies appear as spikes. A possible approach to transform the residual values into probabilistic scores is to learn the distribution of the residual values. For instance, the algorithm proposed in [Siffer et al., 2017] which employs extreme value theory can be used to infer the distribution of the residual values. Another approach is to apply an anomaly detection algorithm which generates probabilistic scores (e.g., LSSM) to the generated residual values. In all the presented experiments, we report the results for a model called LRPE which is the combination of RPE and LSSM, i.e., LSSM is applied to the output of the RPE algorithm. Since we could not fit the results of all the models in a table, we report the results of LRPE in each section inside the text.

A. Performance analysis with synthetic data

In this experiment, we use synthetic data with a seasonal pattern to evaluate the performance of the algorithms. All the time-series used in this experiment are generated as

$$\mathbf{t}(j) = \sum_{k=1}^4 z_k \cos(2\pi\omega_k j + \psi_k) + \mathbf{n}(j).$$

For each time-series $1/\omega_1$ is sampled randomly from (40, 70), $1/\omega_2$ is sampled randomly from (20, 40), $1/\omega_3$ is sampled randomly from (10, 20), and $1/\omega_4$ is sampled randomly from (2, 6). The phases $\{\psi_k\}_{k=1}^4$ are sampled randomly from $(0, 2\pi)$. We assigned higher weights to the components with lower frequency. Specifically, we used $[z_1, z_2, z_3, z_4] = [2, 1.6, 1.2, 0.8]$. The first two (from right) time-series of Figure 1 shows two examples of the generated time-series. In all the experiments with synthetic data, 4 % of the time-stamps of each time-series are anomalies and results are obtained as the average of 20 independent runs. In each run, we obtain max- F_1 accuracy along with its corresponding precision and recall. In all the tables, F_1 , P, and R refer to max- F_1 , precision, and recall, respectively.

1) *Detecting Contextual Anomalies:* In this experiment, we examine the ability of the algorithms in detecting anomalies whose amplitude such that they do not necessarily push the time-stamp value out of the range of normal values. Table I and Table II show the performance of the algorithms for two scenarios where the amplitude of the added point anomalies are equal to $f/2$ and f where $f = (\beta_{0.9} - \beta_{0.1})$ and β_q is equal to q^{th} quantile of \mathbf{t} . Clearly, detecting the anomalies whose amplitude is smaller is more challenging and the algorithm should know the local structure precisely to be able to identify the potential deviations. One can observe that in both cases, RPE yields the best performance which suggests that RPE is accurately aware of the local structure of the time-series. The obtained results for LRPE corresponding to the scenarios in Table I and Table II are ($F_1=0.99$, $P=0.99$, $R=0.99$) and ($F_1=0.95$, $P=0.95$, $R=0.99$), respectively. Figure 4 shows an example where the time-series contains several contextual anomalies.

Remark 6. *The reported F_1 -score, precision, and recall are the average of F_1 -score, precision, and recall of 20 independent runs. Therefore, the reported F_1 -score is not necessarily equal to the harmonic mean of the reported precision and recall.*

2) *Identifying range anomalies:* In this experiment, we investigate the performance of the models when the length of each anomaly is more than a single time-stamp. Table III shows the performance of the models when each anomaly corrupts 2 consecutive time-stamps and Table IV shows the results when each anomaly corrupts 4 consecutive time-stamps. In both cases, the amplitude of the added anomalies is equal to $f/1.5$ and the standard deviation of the added noise is equal to 0.1. One can observe that the performance of all the algorithms degrade when the range of anomalies increases in time domain and in

TABLE I

ACCURACY OF THE ALGORITHMS. ANOMALY AMPLITUDE EQUAL TO f (EXPERIMENT V-A1).

	RCF	RPE	SPE	IID	SR	AR	LSSM
F_1	0.74	1	0.96	0.64	0.81	0.97	0.93
P	0.86	1	0.95	0.79	0.85	0.99	0.9
R	0.68	1	0.96	0.58	0.80	0.96	0.98

TABLE II

ACCURACY OF THE ALGORITHMS. ANOMALY AMPLITUDE EQUAL TO $f/2$ (EXPERIMENT V-A1).

	RCF	RPE	SPE	IID	SR	AR	LSSM
F_1	0.42	0.96	0.92	0.25	0.38	0.86	0.55
P	0.52	0.96	0.92	0.36	0.54	0.86	0.63
R	0.43	0.98	0.92	0.33	0.37	0.89	0.60

both cases RPE yields the best accuracy. The obtained results for LRPE corresponding to the scenarios in Table III and Table IV are ($F_1=0.94$, $P=0.98$, $R=0.91$) and ($F_1=0.83$, $P=0.82$, $R=0.87$), respectively.

TABLE III

THE LENGTH OF EACH ANOMALY EQUAL TO 2 TIME-STAMPS. (EXPERIMENT V-A2).

	RCF	RPE	SPE	IID	SR	AR	LSSM
F_1	0.5	0.97	0.77	0.40	0.43	0.93	0.66
P	0.67	0.98	0.85	0.46	0.63	0.96	0.68
R	0.48	0.96	0.74	0.49	0.4	0.91	0.67

TABLE IV

THE LENGTH OF EACH ANOMALY EQUAL TO 4 TIME-STAMPS. (EXPERIMENT V-A2).

	RCF	RPE	SPE	IID	SR	AR	LSSM
F_1	0.51	0.83	0.55	0.42	0.33	0.76	0.5
P	0.59	0.81	0.59	0.44	0.52	0.80	0.63
R	0.63	0.87	0.59	0.68	0.43	0.79	0.51

TABLE V
ACCURACY OF THE ALGORITHMS. REAL TIME-SERIES SAMPLED FROM YAHOO DATASET (EXPERIMENT V-B).

	RCF	RPE	SPE	IID	SR	AR	LSSM
F_1	0.72	0.88	0.77	0.72	0.72	0.79	0.84
P	0.77	0.92	0.87	0.88	0.86	0.89	0.85
R	0.72	0.88	0.74	0.66	0.67	0.74	0.87

B. Experiment with real data: Yahoo

In this experiment, we use the real time-series in the Yahoo dataset. Yahoo dataset is an open data for anomaly detection released by Yahoo. The real time-series in the Yahoo dataset are long (mostly around 1400 time-stamps) and in order to create challenging/realistic scenarios, we sample random subsequences from each time-series with length 300 where the first 100 time-stamps were used as training data (if the frequency is 1 day, one needs to wait for about 4 years to collect 1400 samples!). Specifically, for each real time-series, we sampled 15 random sub-time-series with length equal to 300. Since these sub-time-series might not include any anomaly, we added anomalies to each sampled time-series to ensure that 4 % of the time-stamps are anomalies (we used similar technique used for the synthetic data to add anomalies to the real time-series and half of the added anomalies were contextual anomalies). Table V shows the accuracy of different models and the obtained results for LRPE are ($F_1=0.86$, $P=0.93$, $R=0.83$). One can observe that RPE yields the best accuracy among the models. The main reason is that the robust projection step enables the RPE algorithm to robustly compute the residual values even if its window contains corrupted time-stamps. In addition, it enables the algorithm to distinguish the outlying time-stamps even if they are close to each.

Remark. Similar experiments with two more real dataset are included in the appendix.

C. Choosing window size M_1

The main idea behind the RPE algorithm was to utilize the low dimensional structure of the trajectory matrix $\mathbf{X} \in \mathbb{R}^{M_1 \times M_2}$ to robustly extract the outlying components using the column space of \mathbf{X} . Therefore, M_1 should be sufficiently large such that \mathbf{X} is a low rank matrix. The presented theoretical results also emphasised that r/M_1 should be sufficiently small to guarantee the performance of the robust projection step because the value of $\mu(\mathbf{U})$ increases in most cases when r/M_1 increases (for instance, for a randomly generated subspace $\mathbf{U} \in \mathbb{R}^{M_1 \times r}$, $\mathbb{E}(\|\mathbf{e}_i^T \mathbf{U}\|_2^2) = \frac{r}{M_1}$ [Candès and Recht, 2009]). In the real and synthetic time-series that we studied, the ranks of the time-series which contained temporal background signal

were smaller than 6 in most of the cases. Therefore, we chose $M_1 = 30$ in the presented experiments which means that the dimension of the matrix is at least 5 times larger than the rank. If there is not a known upper-bound for r , one can form multiple trajectory matrices with different values of M_1 and find the proper value which ensures that \mathbf{X} is a low rank matrix.

Although M_1 should be sufficiently large to ensure that r/M_1 is small enough, choosing M_1 too large also hurt the performance of the model because $M_2 = n - 1 - M_1$ where M_2 is the number of columns of \mathbf{X} and a large window size makes M_2 small. Note that in order to ensure that \mathbf{X} is a low rank matrix, both M_1 and M_2 should be sufficiently larger than r . Moreover, choosing a very large value for M_1 can limit the understanding of the model from the local structures of the time-series. Our investigations suggest that choosing $5r \leq M_1 \leq 10r$ works best. For instance, Table VI shows the performance of RPE for a scenario similar to the experiment in Section V-A2 (length of range anomalies equal to 2) where the length of the training time-series is equal to 100. The results show that choosing a too small or a too large value for M_1 degrade the performance and the performance is not sensitive to the value of M_1 as long as we choose a reasonable value.

TABLE VI
THE ACCURACY OF RPE WITH DIFFERENT VALUES OF M_1 (EXPERIMENT V-C).

M_1	30	40	50	10	90
F_1	0.97	0.98	0.98	0.42	0.68

VI. CONCLUSION

A novel, closed-form, and efficient anomaly detection algorithm for univariate time-series were proposed. The proposed method, dubbed RPE, leverages the linear structure of the trajectory matrix and it employs a robust projection method to identify the corrupted time-stamps. A provable and closed-form algorithm was presented which enables the algorithm to perform the robust projection step without the need to run an iterative solver for each time-stamp. The presented experiments showed that RPE can outperform the existing approaches with a notable margin.

REFERENCES

- [Braei and Wagner, 2020] Braei, M. and Wagner, S. (2020). Anomaly detection in univariate time-series: A survey on the state-of-the-art. *arXiv preprint arXiv:2004.00433*.

- [Candès et al., 2011] Candès, E. J., Li, X., Ma, Y., and Wright, J. (2011). Robust principal component analysis? *Journal of the ACM (JACM)*, 58(3):1–37.
- [Candès and Recht, 2009] Candès, E. J. and Recht, B. (2009). Exact matrix completion via convex optimization. *Foundations of Computational mathematics*, 9(6):717–772.
- [Candes and Tao, 2005] Candès, E. J. and Tao, T. (2005). Decoding by linear programming. *IEEE transactions on information theory*, 51(12):4203–4215.
- [Challu et al., 2022] Challu, C., Jiang, P., Wu, Y. N., and Callot, L. (2022). Deep generative model with hierarchical latent factors for time series anomaly detection. *Proceedings of the 25th International Conference on Artificial Intelligence and Statistics (AISTATS)*. PMLR: Volume 151.
- [Chandola, 2009] Chandola, V. (2009). *Anomaly detection for symbolic sequences and time series data*. University of Minnesota.
- [Chandrasekaran et al., 2011] Chandrasekaran, V., Sanghavi, S., Parrilo, P. A., and Willsky, A. S. (2011). Rank-sparsity incoherence for matrix decomposition. *SIAM Journal on Optimization*, 21(2):572–596.
- [Dokumentov et al., 2014] Dokumentov, A., Hyndman, R. J., et al. (2014). Low-dimensional decomposition, smoothing and forecasting of sparse functional data. *Technical report, Monash University*.
- [Durbin and Koopman, 2012] Durbin, J. and Koopman, S. J. (2012). *Time series analysis by state space methods*. Oxford university press.
- [Feng et al., 2013] Feng, J., Xu, H., and Yan, S. (2013). Online robust pca via stochastic optimization. *Advances in neural information processing systems*, 26:404–412.
- [Gillard and Usevich, 2018] Gillard, J. and Usevich, K. (2018). Structured low-rank matrix completion for forecasting in time series analysis. *International Journal of Forecasting*, 34(4):582–597.
- [Golyandina et al., 2001] Golyandina, N., Nekrutkin, V., and Zhigljavsky, A. A. (2001). *Analysis of time series structure: SSA and related techniques*. CRC press.
- [Guha et al., 2016] Guha, S., Mishra, N., Roy, G., and Schrijvers, O. (2016). Robust random cut forest based anomaly detection on streams. In *International conference on machine learning*, pages 2712–2721. PMLR.
- [Hundman et al., 2018] Hundman, K., Constantinou, V., Laporte, C., Colwell, I., and Soderstrom, T. (2018). Detecting spacecraft anomalies using lstms and nonparametric dynamic thresholding. In *Proceedings of the 24th ACM SIGKDD international conference on knowledge discovery & data mining*, pages 387–395.
- [Jin et al., 2017] Jin, Y., Qiu, C., Sun, L., Peng, X., and Zhou, J. (2017). Anomaly detection in time series via robust pca. In *2017 2nd IEEE International Conference on Intelligent Transportation Engineering (ICITE)*, pages 352–355. IEEE.
- [Karrila et al., 2011] Karrila, S., Lee, J. H. E., and Tucker-Kellogg, G. (2011). A comparison of methods for data-driven cancer outlier discovery, and an application scheme to semisupervised predictive biomarker discovery. *Cancer informatics*, 10:CIN–S6868.
- [Khan and Poskitt, 2017] Khan, M. A. R. and Poskitt, D. (2017). Forecasting stochastic processes using singular spectrum analysis: Aspects of the theory and application. *International Journal of Forecasting*, 33(1):199–213.
- [Kruegel and Vigna, 2003] Kruegel, C. and Vigna, G. (2003). Anomaly detection of web-based attacks. In *Proceedings of the 10th ACM conference on Computer and communications security*, pages 251–261.
- [Lerman and Maunu, 2018] Lerman, G. and Maunu, T. (2018). Fast, robust and non-convex subspace recovery. *Information and Inference: A Journal of the IMA*, 7(2):277–336.
- [Lois and Vaswani, 2015] Lois, B. and Vaswani, N. (2015). Online matrix completion and online robust pca. In *2015 IEEE International Symposium on Information Theory (ISIT)*, pages 1826–1830. IEEE.

- [Munir et al., 2018] Munir, M., Siddiqui, S. A., Dengel, A., and Ahmed, S. (2018). Deepant: A deep learning approach for unsupervised anomaly detection in time series. *Ieee Access*, 7:1991–2005.
- [Papailias and Thomakos, 2017] Papailias, F. and Thomakos, D. (2017). Exssa: Ssa-based reconstruction of time series via exponential smoothing of covariance eigenvalues. *International Journal of Forecasting*, 33(1):214–229.
- [Raginsky et al., 2012] Raginsky, M., Willett, R. M., Horn, C., Silva, J., and Marcia, R. F. (2012). Sequential anomaly detection in the presence of noise and limited feedback. *IEEE Transactions on Information Theory*, 58(8):5544–5562.
- [Rahmani and Atia, 2017a] Rahmani, M. and Atia, G. K. (2017a). Coherence pursuit: Fast, simple, and robust principal component analysis. *IEEE Transactions on Signal Processing*, 65(23):6260–6275.
- [Rahmani and Atia, 2017b] Rahmani, M. and Atia, G. K. (2017b). High dimensional low rank plus sparse matrix decomposition. *IEEE Transactions on Signal Processing*, 65(8):2004–2019.
- [Rahmani and Li, 2019] Rahmani, M. and Li, P. (2019). Outlier detection and robust pca using a convex measure of innovation. *Advances in Neural Information Processing Systems*, 32.
- [Rahmani and Li, 2021] Rahmani, M. and Li, P. (2021). Fast and provable robust pca via normalized coherence pursuit. In *ICASSP 2021-2021 IEEE International Conference on Acoustics, Speech and Signal Processing (ICASSP)*, pages 5305–5309. IEEE.
- [Ren et al., 2019] Ren, H., Xu, B., Wang, Y., Yi, C., Huang, C., Kou, X., Xing, T., Yang, M., Tong, J., and Zhang, Q. (2019). Time-series anomaly detection service at microsoft. In *Proceedings of the 25th ACM SIGKDD International Conference on Knowledge Discovery & Data Mining*, pages 3009–3017.
- [Shen et al., 2020] Shen, L., Li, Z., and Kwok, J. (2020). Timeseries anomaly detection using temporal hierarchical one-class network. *Advances in Neural Information Processing Systems*, 33:13016–13026.
- [Siffer et al., 2017] Siffer, A., Fouque, P.-A., Termier, A., and Largouet, C. (2017). Anomaly detection in streams with extreme value theory. In *Proceedings of the 23rd ACM SIGKDD International Conference on Knowledge Discovery and Data Mining*, pages 1067–1075.
- [Su et al., 2019] Su, Y., Zhao, Y., Niu, C., Liu, R., Sun, W., and Pei, D. (2019). Robust anomaly detection for multivariate time series through stochastic recurrent neural network. In *Proceedings of the 25th ACM SIGKDD International Conference on Knowledge Discovery & Data Mining*, pages 2828–2837.
- [Usevich, 2010] Usevich, K. (2010). On signal and extraneous roots in singular spectrum analysis. *arXiv preprint arXiv:1006.3436*.
- [Usevich and Comon, 2016] Usevich, K. and Comon, P. (2016). Hankel low-rank matrix completion: Performance of the nuclear norm relaxation. *IEEE Journal of Selected Topics in Signal Processing*, 10(4):637–646.
- [Wainwright, 2019] Wainwright, M. J. (2019). *High-dimensional statistics: A non-asymptotic viewpoint*, volume 48. Cambridge University Press.
- [Wang et al., 2018] Wang, X., Zhang, Y., Liu, H., Wang, Y., Wang, L., and Yin, B. (2018). An improved robust principal component analysis model for anomalies detection of subway passenger flow. *Journal of advanced transportation*, 2018.
- [Xu et al., 2018] Xu, H., Chen, W., Zhao, N., Li, Z., Bu, J., Li, Z., Liu, Y., Zhao, Y., Pei, D., Feng, Y., et al. (2018). Unsupervised anomaly detection via variational auto-encoder for seasonal kpis in web applications. In *Proceedings of the 2018 World Wide Web Conference*, pages 187–196.
- [Zhao et al., 2020] Zhao, H., Wang, Y., Duan, J., Huang, C., Cao, D., Tong, Y., Xu, B., Bai, J., Tong, J., and Zhang, Q. (2020). Multivariate time-series anomaly detection via graph attention network. In *2020 IEEE International Conference on Data Mining (ICDM)*, pages 841–850. IEEE.

[Zhou et al., 2019] Zhou, B., Liu, S., Hooi, B., Cheng, X., and Ye, J. (2019). Beatgan: Anomalous rhythm detection using adversarially generated time series. In *IJCAI*, pages 4433–4439.

Proofs of the theoretical results

Proof of Lemma 1

In order to show that \mathbf{a} is the optimal point of (5), it is enough to show that

$$\|\mathbf{x} - \mathbf{U}(\mathbf{a} + \mathbf{h})\|_1 - \|\mathbf{x} - \mathbf{U}\mathbf{a}\|_1 > 0 \quad (10)$$

for any sufficiently small non-zero perturbation vector \mathbf{h} . Note that $\mathbf{x} = \mathbf{U}\mathbf{a} + \mathbf{s}$ which means that (10) can be simplified as

$$\sum_{i \in \mathcal{I}_s} |\mathbf{s}(i) - \mathbf{u}_i^T \mathbf{h}| + \sum_{i \notin \mathcal{I}_s} |\mathbf{u}_i^T \mathbf{h}| - \sum_{i \in \mathcal{I}_s} |\mathbf{s}(i)| > 0, \quad (11)$$

where \mathcal{I}_s is the set of the indices of the non-zero elements of \mathbf{s} . According to (11), it suffices to ensure that

$$\sum_{i \notin \mathcal{I}_s} |\mathbf{u}_i^T \mathbf{h}| - \sum_{i \in \mathcal{I}_s} |\mathbf{u}_i^T \mathbf{h}| > 0, \quad (12)$$

which is equivalent to guaranteeing that

$$\|\mathbf{U}\mathbf{h}\|_1 - 2 \sum_{i \in \mathcal{I}_s} |\mathbf{u}_i^T \mathbf{h}| > 0. \quad (13)$$

Since \mathbf{h} appears on both sides of (13), it is enough to ensure that

$$\min_{\mathbf{h} \in \mathbb{S}^{r-1}} \|\mathbf{U}\mathbf{h}\|_1 - 2 \sum_{i \in \mathcal{I}_s} \|\mathbf{u}_i\|_2 > 0. \quad (14)$$

Therefore, according to the definition of μ

$$\mu^2(\mathbf{U}) = \max_i \frac{\|\mathbf{e}_i^T \mathbf{U}\|_2^2}{r},$$

where \mathbf{e}_i is the i^{th} column/row of the identity matrix, it is enough to ensure that

$$\min_{\mathbf{h} \in \mathbb{S}^{r-1}} \|\mathbf{U}\mathbf{h}\|_1 - 2m\sqrt{r}\mu(\mathbf{U}) > 0. \quad (15)$$

Thus, if $\kappa(\mathbf{U}) < \frac{1}{2m\sqrt{r}}$, then (10) is guaranteed to hold which means that \mathbf{a} is the optimal point of (5) where $\kappa(\mathbf{U}) = \mu(\mathbf{U})\gamma(\mathbf{U})$ and $\gamma(\mathbf{U}) = \frac{1}{\min_{\mathbf{h} \in \mathbb{S}^{r-1}} \|\mathbf{U}\mathbf{h}\|_1}$.

Proof of Lemma 2

The vector of residual values $\hat{\mathbf{e}} = |\mathbf{x} - \mathbf{U}\mathbf{U}^T \mathbf{x}|$ can be written as $\hat{\mathbf{e}} = |\mathbf{U}^\perp \mathbf{U}^{\perp T} \mathbf{x}|$ where $\mathbf{U}^\perp \in \mathbb{R}^{M_1 \times (M_1 - r)}$ is an orthonormal basis for the complement of the span of \mathbf{U} . Define \mathcal{I}_s as the set of the indices of the non-zero elements of \mathbf{s} . The vector $\hat{\mathbf{e}} \in \mathbb{R}^{M_1}$ can be written as

$$\hat{\mathbf{e}} = \left| \mathbf{U}^\perp \sum_{j \in \mathcal{I}_s} \mathbf{s}(j) \mathbf{u}_j^\perp \right|, \quad (16)$$

where $s(j)$ is the j^{th} element of \mathbf{s} and \mathbf{u}_j^\perp is the j^{th} row of \mathbf{U}^\perp . Therefore, the i^{th} element of $\hat{\mathbf{e}}$ can be described as

$$\hat{\mathbf{e}}(i) = \left| \sum_{j \in \mathcal{I}_s} s(j) \mathbf{u}_i^{\perp T} \mathbf{u}_j^\perp \right|. \quad (17)$$

Since \mathbf{U}^\perp is the span of the complement of the span of \mathbf{U} and they both are orthonormal matrices, we can conclude that

$$\begin{aligned} \mathbf{u}_i^{\perp T} \mathbf{u}_j^\perp &= -\mathbf{u}_i^T \mathbf{u}_j \quad \text{if } i \neq j \\ \mathbf{u}_i^{\perp T} \mathbf{u}_i^\perp &= 1 - \mathbf{u}_i^T \mathbf{u}_i \end{aligned} \quad (18)$$

where \mathbf{u}_i is the i^{th} row of \mathbf{U} . Now we consider different scenarios for $\hat{\mathbf{e}}(i)$. When $i \notin \mathcal{I}_s$

$$\hat{\mathbf{e}}(i) = \left| \sum_{j \in \mathcal{I}_s} s(j) \mathbf{u}_i^{\perp T} \mathbf{u}_j^\perp \right| = \left| - \sum_{j \in \mathcal{I}_s} s(j) \mathbf{u}_i^T \mathbf{u}_j \right|, \quad (19)$$

and when $i \in \mathcal{I}_s$

$$\hat{\mathbf{e}}(i) = \left| \sum_{j \in \mathcal{I}_s} s(j) \mathbf{u}_i^{\perp T} \mathbf{u}_j^\perp \right| = \left| s(i) - s(i) \mathbf{u}_i^T \mathbf{u}_i - \sum_{\substack{j \in \mathcal{I}_s \\ j \neq i}} s(j) \mathbf{u}_i^T \mathbf{u}_j \right|. \quad (20)$$

According to the definition of $\mu(\mathbf{U})$,

$$\mathbf{u}_i^T \mathbf{u}_j \leq r \mu^2(\mathbf{U}).$$

Therefore, when $i \notin \mathcal{I}_s$, we can set the following upper-bound for $\hat{\mathbf{e}}(i)$

$$\hat{\mathbf{e}}(i) = \left| - \sum_{j \in \mathcal{I}_s} s(j) \mathbf{u}_i^T \mathbf{u}_j \right| \leq r \mu^2(\mathbf{U}) \sum_{j \in \mathcal{I}_s} |s(j)| \quad (21)$$

and the following lower-bound for $i \in \mathcal{I}_s$

$$\begin{aligned} \hat{\mathbf{e}}(i) &= \left| s(i) - s(i) \mathbf{u}_i^T \mathbf{u}_i - \sum_{\substack{j \in \mathcal{I}_s \\ j \neq i}} s(j) \mathbf{u}_i^T \mathbf{u}_j \right| \\ &\geq |s(i)| - \sum_{j \in \mathcal{I}_s} |s(j) \mathbf{u}_i^T \mathbf{u}_j| \geq |s(i)| - r \mu^2(\mathbf{U}) \sum_{j \in \mathcal{I}_s} |s(j)|. \end{aligned} \quad (22)$$

According to (21) and (22), in order to ensure that the algorithm samples all the corrupted time-stamps, it is enough to guarantee that

$$\mu^2(\mathbf{U}) \leq \frac{1}{2r} \frac{\min_i \zeta_i}{\sum_j \zeta_j}, \quad (23)$$

where $\{\zeta_i\}_{i=1}^m$ are the absolute value of the non-zero elements of \mathbf{s} and $m = |\mathcal{I}_s|$.

Proof of Theorem 4

In order to prove Theorem 4, first we derive the sufficient condition which guarantees that

$$\min_{i \in \mathcal{I}_s} \hat{\mathbf{e}}(i) > \max_{i \notin \mathcal{I}_s} \hat{\mathbf{e}}(i). \quad (24)$$

When the observation vector \mathbf{x} contains added noise, then similar to (16), $\hat{\mathbf{e}}$ can be written as

$$\hat{\mathbf{e}} = \left| \mathbf{U}^\perp \left(\sum_{j \in \mathcal{I}_s} \mathbf{s}(j) \mathbf{u}_j^\perp + \sum_{k=1}^{M_1} \mathbf{n}(k) \mathbf{u}_k^\perp \right) \right|. \quad (25)$$

Thus, the i^{th} element of $\hat{\mathbf{e}}$ can be expanded as follows

$$\hat{\mathbf{e}}(i) = \left| \sum_{j \in \mathcal{I}_s} \mathbf{s}(j) \mathbf{u}_i^{\perp T} \mathbf{u}_j^\perp + \sum_{k=1}^{M_1} \mathbf{n}(k) \mathbf{u}_i^{\perp T} \mathbf{u}_k^\perp \right|. \quad (26)$$

Similar to the proof of Lemma 2, we set a lower bound for $\hat{\mathbf{e}}(i)$ when $i \in \mathcal{I}_s$ and an upper-bound for $\hat{\mathbf{e}}(i)$ when $i \notin \mathcal{I}_s$. The upper-bound for the cases where $i \notin \mathcal{I}_s$ can be obtained as

$$\begin{aligned} \hat{\mathbf{e}}(i) &= \left| \sum_{j \in \mathcal{I}_s} \mathbf{s}(j) \mathbf{u}_i^{\perp T} \mathbf{u}_j^\perp + \sum_{k=1}^{M_1} \mathbf{n}(k) \mathbf{u}_i^{\perp T} \mathbf{u}_k^\perp \right| \\ &\leq \sum_{j \in \mathcal{I}_s} \left| \mathbf{s}(j) \mathbf{u}_i^{\perp T} \mathbf{u}_j^\perp \right| + \left| \sum_{k=1}^{M_1} \mathbf{n}(k) \mathbf{u}_i^{\perp T} \mathbf{u}_k^\perp \right| \end{aligned} \quad (27)$$

We did not specify any distribution for the added noise vector \mathbf{n} but we made the following two assumptions

$$\begin{aligned} \mathbb{P} [|\mathbf{n}(k)| > \eta] &< \delta/M_1 \\ \mathbb{P} [|\mathbf{n}(k)| > 0] &= \mathbb{P} [|\mathbf{n}(k)| < 0]. \end{aligned} \quad (28)$$

In order to bound the second part of (27), we utilize the Hoeffding's inequality [Wainwright, 2019].

Lemma 5. *Suppose that $\{x_i\}_{i=1}^m$ are bounded random variables such that $a \leq x_i \leq b$ and assume that $\{\epsilon_i\}_{i=1}^m$ are sampled independently from the Rademacher distribution. Then,*

$$\mathbb{P} \left[\left| \sum_{i=1}^m \epsilon_i x_i \right| > t \right] < \exp \left(-\frac{2t^2}{m(b-a)^2} \right). \quad (29)$$

Since $\mathbb{P} [|\mathbf{n}(k)| > 0] = \mathbb{P} [|\mathbf{n}(k)| < 0]$, the distribution of

$$\left| \sum_{k=1}^{M_1} \mathbf{n}(k) \mathbf{u}_i^{\perp T} \mathbf{u}_k^\perp \right|$$

is equivalent to the distribution of $\left| \sum_{k=1}^{M_1} \epsilon_i \mathbf{n}(k) \mathbf{u}_i^\perp{}^T \mathbf{u}_j^\perp \right|$ where $\{\epsilon_i\}_{i=1}^{M_1}$ are sampled independently from Rademacher distribution. Therefore, using Lemma 5 and conditioned on $\mathbf{n}(k) < \eta$, we can conclude that

$$\mathbb{P} \left[\left| \sum_{k=1}^{M_1} \mathbf{n}(k) \mathbf{u}_i^\perp{}^T \mathbf{u}_j^\perp \right| > t \right] \leq \exp \left(-\frac{2t^2}{M_1 \mu^4(\mathbf{U}) r^2 \eta^2} \right), \quad (30)$$

where we used the fact that $|\mathbf{u}_i^\perp{}^T \mathbf{u}_j^\perp| = |\mathbf{u}_i^T \mathbf{u}_j|$ when $i \neq j$. Thus, according to (30) and the presumed model for noise,

$$\mathbb{P} \left[\left| \sum_{k=1}^{M_1} \mathbf{n}(k) \mathbf{u}_i^\perp{}^T \mathbf{u}_j^\perp \right| > r \mu^2(\mathbf{U}) \eta \sqrt{\frac{M_1 \log 1/\delta}{2}} \right] \leq 2\delta. \quad (31)$$

Using (27) and (31) we can establish the following upper-bound for $\hat{\mathbf{e}}(i)$ for the cases where $i \notin \mathcal{I}_s$

$$\mathbb{P} \left[\hat{\mathbf{e}}(i) < r \mu^2(\mathbf{U}) \sum_{j=1}^m \zeta_j + r \mu^2(\mathbf{U}) \eta \sqrt{\frac{M_1 \log 1/\delta}{2}} \right] \geq 1 - 2\delta, \quad (32)$$

where $\{\zeta_i\}_{i=1}^m$ are the absolute value of the non-zero elements of \mathbf{s} and $m = |\mathcal{I}_s|$. When $i \in \mathcal{I}_s$, similar to (20), we can rewrite $\hat{\mathbf{e}}(i)$ as

$$\begin{aligned} \hat{\mathbf{e}}(i) &= \left| \mathbf{s}(i) - \mathbf{s}(i) \mathbf{u}_i^T \mathbf{u}_i - \sum_{\substack{j \in \mathcal{I}_s \\ j \neq i}} \mathbf{s}(j) \mathbf{u}_i^T \mathbf{u}_j - \sum_k \mathbf{n}(k) \mathbf{u}_i^T \mathbf{u}_j \right| \\ &\geq |\mathbf{s}(i)| - \left| \sum_{j \in \mathcal{I}_s} \mathbf{s}(j) \mathbf{u}_i^T \mathbf{u}_j \right| - \left| \sum_k \mathbf{n}(k) \mathbf{u}_i^T \mathbf{u}_j \right|. \end{aligned} \quad (33)$$

Using similar techniques used to establish (32) and according to (33), we can conclude that

$$\begin{aligned} \hat{\mathbf{e}}(i) &\geq |\mathbf{s}(i)| - \sum_{j \in \mathcal{I}_s} |\mathbf{s}(j) \mathbf{u}_i^T \mathbf{u}_j| - \left| \sum_k \mathbf{n}(k) \mathbf{u}_i^T \mathbf{u}_j \right| \\ &\geq |\mathbf{s}(i)| - r \mu^2(\mathbf{U}) \sum_j \zeta_j - r \mu^2(\mathbf{U}) \eta \sqrt{\frac{M_1 \log 1/\delta}{2}} \end{aligned} \quad (34)$$

with probability at least $1 - 2\delta$. Thus, according to (32) and (34), we can conclude that if

$$\mu^2(\mathbf{U}) \left(1 + \frac{\eta}{\sum_j \zeta_j} \sqrt{\frac{M_1 \log 1/\delta}{2}} \right) \leq \frac{1}{2r} \frac{\min_j \zeta_j}{\sum_j \zeta_j}, \quad (35)$$

then all the indices of the non-zero elements of \mathbf{s} are successfully rejected by the algorithm.